ISBN: 978-3-95450-227-1 ISSN: 2673-5490 doi:10.18429/JACoW-IPAC2022-MOPOTK053

RLAs WITH FFA ARCS FOR PROTONS AND ELECTRONS*

V. S. Morozov†, Oak Ridge National Lab, Oak Ridge, TN, USA
J. F. Benesch, R. M. Bodenstein, S. A. Bogacz, A. M. Coxe, K. E. Deitrick, D. R. Douglas, B. R. Gamage, G. A. Krafft, K.E. Price, Y. Roblin, A. Seryi, Jefferson Lab, Newport News, VA, USA
J. S. Berg, S. J. Brooks, F. Meot, D. Trbojevic, Brookhaven National Lab, Upton, NY, USA
G. H. Hoffstaetter, Cornell University, Ithaca, NY, USA

Abstract

Recirculating Linear Accelerators (RLAs) provide an efficient way of producing high-power, high-quality, continuous-wave hadron and lepton beams. However, their attractiveness had been limited by the cumbersomeness of multiple recirculating arcs and by the complexity of the spreader and recombiner regions. The latter problem sets one of the practical limitations on the maximum number of recirculations. We present an RLA design concept where the problem of multiple arcs is solved using the Fixed-Field Alternating gradient (FFA) design as in CBETA. The spreader/recombiner design is greatly simplified using an adiabatic matching approach. It allows for the spreader/recombiner function to be accomplished by a single beam line. The concept is applied to the designs of a high-power hadron accelerator being considered at ORNL and a CEBAF electron energy doubling project, FFA@CEBAF, being developed at Jefferson lab.

HIGH-POWER HADRON ACCELERATOR DESIGN STUDY AT ORNL

Introduction

Recent advances in the SRF technology allow for increasingly more reliable and higher power hadron linacs. Due to slow increase of the proton velocity and each RF structure being efficient only in a narrow range of velocities, hadron linear accelerators require several SRF cavity types to cover these ranges and a large number of cavities in total. There are multiple projects in all parts of the world that are already being constructed or proposed [1]. The number of different types of accelerating structures used by these projects varies from 4 to 7. Figure 1 summarizes the beam energy gain per cavity for all types of cavities against their velocity ranges for seven typical projects, namely, SNS [2], ESS [3], MYRRHA [4], Project-X [5], JAEA ADS [6], CiADS [7], and HC HP-SPL [8, 9]. Notably, all of these and other explored projects are straight linacs.

The data in Fig. 1 is described well by the exponential fit

$$\frac{\Delta E}{cav} = 0.6 \exp\left(\frac{\beta}{0.26}\right) \left[\frac{\text{MeV}}{\text{cav}}\right] \quad (1)$$

shown by the green solid line. Only SC cavity data was used in the fit, since high-power CW machines tend to have no or short warm accelerating sections after an RFQ. In anticipation of 50% or so further improvement of SRF performance in the next few years, we scale the fit line by a factor of 1.5 and adopt it for our below estimates.

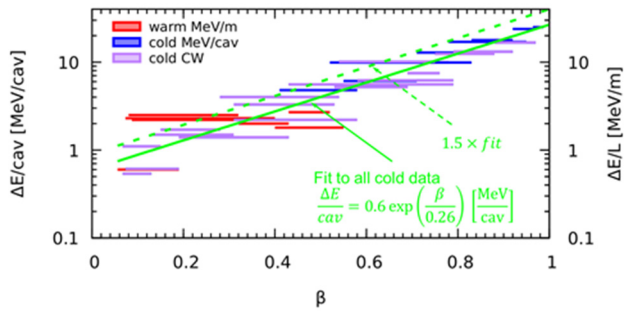

Figure 1: Summary of the energy gains per cavity versus the cavity's velocity range for the seven selected projects. The warm linac data is shown in red on the right vertical scale in terms of the energy gain per unit length.

We next conservatively assume 300 kW for the maximum power that can be coupled into a cavity for all cavity types over the entire relativistic β range. In combination with the extrapolated survey data from Fig. 1, we obtain the optimum current as a function of β

$$I(\beta) = \left[\frac{\Delta P}{cav}\right] \Big/ \left[\frac{\Delta V}{cav}\right](\beta) = 330 \exp\left(-\frac{\beta}{0.26}\right) \text{ [mA]} \quad (2)$$

shown by the green line in Fig. 2.

A point above the green line means that a cavity is running at its power limit but below its maximum voltage while a point below the green line means that a cavity is running at its maximum voltage but below the maximum power that can be made available to it. The magenta line in Fig. 2 illustrates the operation regime of a straight 1 GeV 10 MW proton linac of particular interest for the Accelerator-Driven Subcritical reactor application. Clearly, it is far from the optimum line.

Concept

The power bottleneck set by the high-β cavities in a straight linac is overcome by recirculating the beam through the lower-energy sections up to their cavity power limits. The energy boundaries shown by the red vertical lines in Fig. 2 are chosen so that each section doubles the beam momentum. This is a comfortable parameter range for an FFA arc design as shown later. Under these assumptions, the number of SRF cavities in an RLA design can be

* Authored in part by UT-Battelle, LLC, LDRD, LOIS 10908, under Contract No. DE-AC05-00OR22725, Jefferson Science Associates, LLC under Contract No. DE-AC05-06OR23177, and Brookhaven Science Associates, LLC under Contract No. DE-SC0012704 with the US Department of Energy (DOE).
† morozovvs@ornl.gov

ISBN: 978-3-95450-227-1 ISSN: 2673-5490 doi:10.18429/JACoW-IPAC2022-MOPOTK053

reduced by about a factor of 4 compared to a straight linac design.

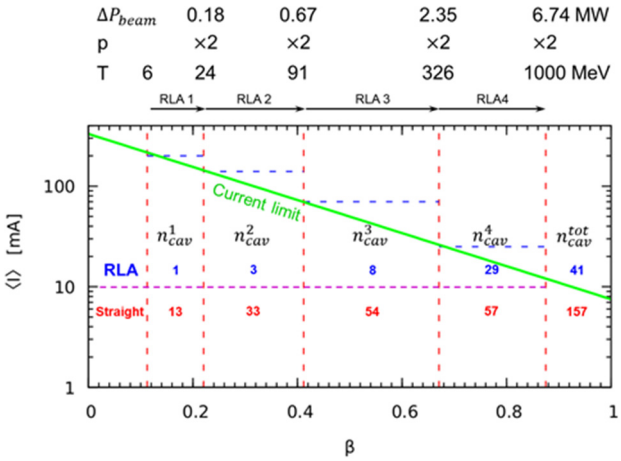

Figure 2: Optimum current (solid green line), current through a cavity in the case of a straight linac (dashed magenta line), and current through a cavity in the case of recirculation (dashed blue lines) as a function of β.

The main problem of recirculating a hadron beam at low-β is the loss of synchronization of the beam with the linac RF and the resulting loss of acceleration efficiency on the 2nd and subsequent turns [10, 11, 12]. This loss is compensated by increase in the number of passes some of which may be inefficient or even decelerating until the goal energy is reached. Low power consumption during the inefficient passes and energy recovery during the decelerating passes keeps the cavity input power under its limit. A more detailed discussion of the linac timing and longitudinal beam match is beyond the scope of this paper.

Table 1: Parameter Scaling of an FFA Cell

Parameter	L	θ	B_y	$\partial B_y/\partial x$	Δx
p	1	1	a	a	1
ρ	a	1	$1/a$	$1/a^2$	x
β (fixed φ)	a	a	1	$1/a^2$	a^2

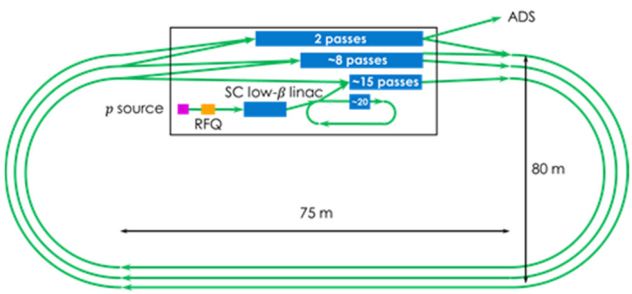

Figure 3: Schematic of a high-power proton accelerator being studied at ORNL.

Multiple recirculations in turn raise the issues of the complexity of having multiple recirculating arcs and matching beam spreaders and recombiners. They are solved using the demonstrated concept [13] of an FFA arcs design and a recent invention of adiabatic FFA match [14]. For the sake of brevity, these ideas are illustrated in application to another project, FFA@CEBAF, discussed later in this paper. Note that there are scaling relations between the FFA cell length (L), bending angle (θ), and bending radius (ρ), the dipole fields (B_y) and field gradients ($\partial B_y/\partial x$) of its magnets, the orbit excursion (Δx), the size of the cell's Twiss β functions, and the beam momentum (p). Some of the basic relations are summarized in Table 1 where φ is the periodic betatron phase per cell. One can apply the relations in Table 1 and their combinations to scale an existing solution to the desired configuration.

Given the above discussion, a preliminary layout of a high-power hadron accelerator investigated at ORNL is depicted by Fig. 3.

FFA@CEBAF

CEBAF Electron Energy Doubling Project

One of the CEBAF upgrade options that have been proposed to further its science is doubling of its energy. Using FFA arcs for additional recirculations of the electron beam through the existing SRF cryomodules is perhaps the most attractive approach to reaching that goal due to its relative simplicity, robustness, compactness, and cost efficiency [15]. It also particularly suitable for the higher energy passes since the FFA absolute momentum acceptance scales with the input momentum with the input to output momentum ratio of up to a factor of about 3. This approach is being explored by the FFA@CEBAF study.

Another advance adopted by FFA@CEBAF that is also applicable to the ORNL design is use of beam line magnets made of permanent magnetic material [16]. When field ramps are not needed as in the FFA design case, they offer multiple advantages over conventional electro-magnetic elements including exceptional compactness, radiation resistance, and achievable field strengths.

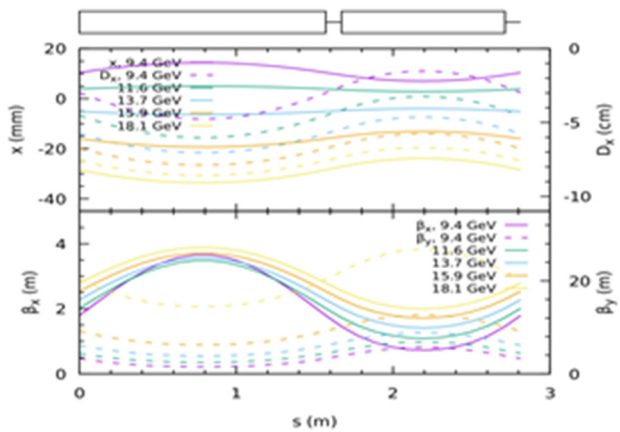

Figure 4: Orbital offest (top, left scale), dispersion (top, right scale) and horizontal (bottom, left scale) and vertical (bottom, right scale) Twiss β functions of a regular periodic cell of the FFA 1 west arc.

Arc Cell

Several design configurations have been explored considering use of permanent combined-function magnets [16]. One of the most efficient configurations as

ISBN: 978-3-95450-227-1 ISSN: 2673-5490 doi:10.18429/JACoW-IPAC2022-MOPOTK053

currently envisioned is a scenario with the addition of two FFAs accelerating the beam in 7.1-18 and 16-23 GeV energy ranges in 5 and 3 passes, respectively. Given the FFA scaling properties summarized in Table 1, here it is sufficient to only focus on the optics design of the west arc of FFA 1 transporting 5 passes of about 9.4, 11.6, 13.5, 15.9, and 18.1 GeV. The magnetic optics of a regular periodic cell of this FFA arc is shown in Fig. 4. It was obtained using the optimized magnet parameters reported in [16]. The optimization ensured that the orbital offset and the beam size corresponding to the optical functions in Fig. 4 are consistent with the aperture attainable with a permanent magnet design at the required magnetic field and its gradient.

At the electron energies of interest, the particle velocity variation is clearly not an issue as in the case of a hadron RLA. The time-of-flight adjustment and longitudinal beam matching are again beyond the scope of this paper.

Straight Cell

CEBAF straights contain relatively long cryomodules with relatively weak focusing elements between them to transport the beam over a wide energy range. This results in the straights having periodic optics solutions with relatively large β functions at high energies as shown in Fig. 5. The design of a periodic straight cell is based on triplet focusing with long drifts around the focusing quadrupoles for placement of SRF cryomodules. The triplet quadrupoles are also assumed to be made of permanent magnetic material.

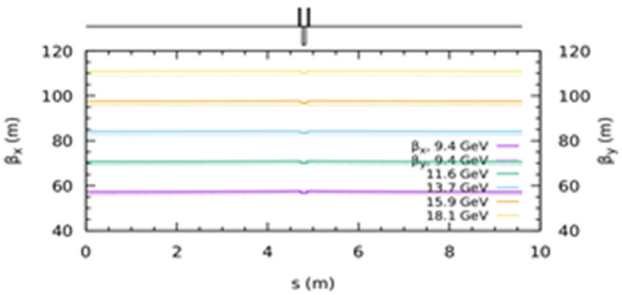

Figure 5: Horizontal (left scale) and vertical (right scale) Twiss β functions of a regular periodic straight cell of FFA 1.

Arc to Straight Matching Sections

It presents a challenge to match the relatively tight optics of the FFA arcs to the large-β periodic triplet optics of the straights. It is done in several steps: a section for *adiabatic suppression of the orbital offset and dispersion*, an *intermediate matching* section, and a *final beam expansion* section.

The design of the adiabatic orbit and dispersion suppression part is based on the adiabatic matching approach [14]. This part of the matching section consists of 26 FFA cells. Their geometry and the quadrupole field strengths are kept fixed while their dipole fields and therefore their bending angles are scaled per the adiabatic approach according to the following polynomial relation

$$\theta_i = \left[1 - f_T\left(\frac{i}{n_T+1}\right)\right]\theta_{arc}\,,\; f_T(x) = 3x^2 - 2x^3\,, \quad (3)$$

where θ_i is the bending angle of ith matching cell, θ_{arc} is the bending angle of a regular arc cell, and n_T is the total number of matching cells. The resulting orbit and optics behavior is shown in Fig. 6. Note the lack of perturbation in the β and therefore constant phase advance per cell.

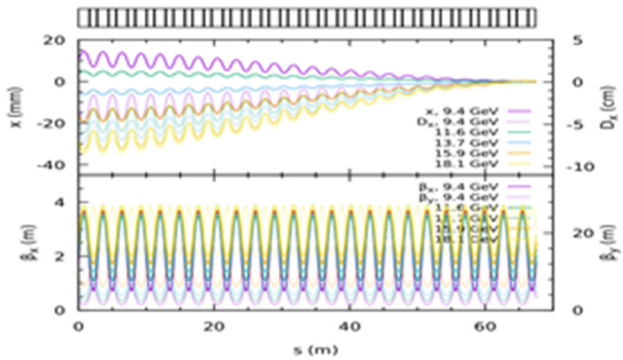

Figure 6: Orbital offest (top, left scale), dispersion (top, right scale) and horizontal (bottom, left scale) and vertical (bottom, right scale) Twiss β functions of the adiabatic part of the matching section.

The adiabatic matching approach has been demonstrated to work well when the phase advance per cell is kept nearly constant. The development of a systematic approach to optimal matching of periodic cells with significantly different periodic betatron phase advances is in progress.

Figure 7 shows a solution for the intermediate and final segments of the matching section obtained by numerical optimization of the magnet strengths to satisfy the Twiss matching constraints. The matching lattice in Fig. 7 consists of 16 straight cells built using same-length magnets as the periodic arc cells that are followed by 10 triplet cells built using same-length magnets as the periodic straight cells. The drift lengths between the triplets are gradually increased according to the polynomial law of Eq. (3). Note the nearly regular behavior of the magnet strengths suggesting that a systematic solution exists.

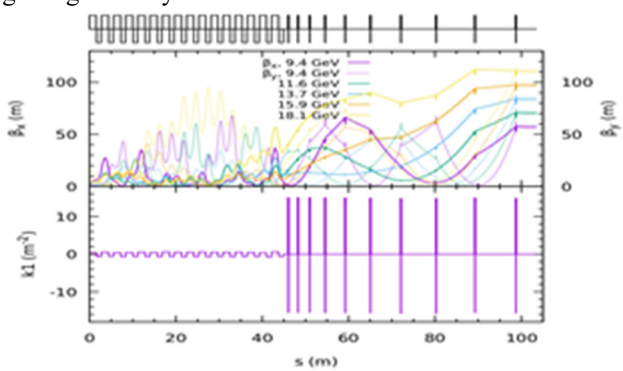

Figure 7: Orbital offest (top, left scale), dispersion (top, right scale) and horizontal (bottom, left scale) and vertical (bottom, right scale) Twiss β functions of the intermiediate and final segments of the matching section.

CONCLUSION

FFA approach to RLA optics design opens new opportunities for efficient designs of hadron and electron accelerators.

ISBN: 978-3-95450-227-1 ISSN: 2673-5490 doi:10.18429/JACoW-IPAC2022-MOPOTK053

REFERENCES

[1] S. H. Kim, "Advances in SRF for Neutron Sources," talk at *15th Int. Conf. RF SC (SRF'11)*, Chicago, IL (2011). http://accel-conf.web.cern.ch/SRF2011/talks/moiob03_talk.pdf

[2] S. Henderson *et al.*, "The Spallation Neutron Source accelerator system design," *Nucl. Instrum. Meth. Sect. A,* vol. 763, pp. 610-673, 2014. https://doi.org/10.1016/j.nima.2014.03.067

[3] K. Andersen *et al.*, "ESS Conceptual Design Report," Rep. No ESS-2012-001, 2012. https://europeanspallation-source.se/sites/default/files/downloads/2017/09/CDR_final_120206.pdf

[4] F. Bouly *et al.*, "Superconducting linac design upgrade in view of the 100 MeV MYRRHA Phase I," in *Proc. IPAC'19*, Melbourne, Australia, May 2019, paper MOPTS003, pp. 837-840, doi:10.18429/JACoW-IPAC2019-MOPTS003

[5] N. Solyak *et al.*, "Physics design of the Project X CW linac," in *Proc. PAC'11*, New York, 2011, paper MOP145, pp. 364-366. https://accelconf.web.cern.ch/PAC2011/papers/mop145.pdf

[6] B. Yee-Rendon *et al.*, "Present Status of the R&D of the Superconducting Linac for the JAEA-ADS", *JPS Conf. Proc., vol.* 33, p. 011043, 2021. doi.org/10.7566/JPSCP.33.011043

[7] S. Liu *et al.*, "Commissioning of China ADS demo Linac and baseline design of CiADS project," *J. Phys.: Conf. Ser.* 1401, p. 012009, 2020. doi.org/10.1088/1742-6596/1401/1/012009

[8] F. Gerigk *et al.*, "Conceptual Design of the Low-Power and High-Power SPL," Rep. No CERN-2014-007, 2014. https://cds.cern.ch/record/1969922/files/CERN-2014-007-SPL.pdf

[9] L. Arnaudon *et al.*, "Linac4 Technical Design Report," Rep. No CERN-AB-2006-084 ABP/RF, 2006. https://cds.cern.ch/record/1004186/files/ab-2006-084.pdf

[10] G.A. Krafft *et al.*, "Measuring and adjusting the path length at CEBAF", in *Proc. PAC'95*, Dallas, TX, USA, May 1995, paper WXE01, p. 2429. doi:10.1109/PAC.1995.505573

[11] E. Yamakawa *et al.*, "Serpentine acceleration in zero-chromatic FFAG accelerators," *Nucl. Instrum. Meth. Sect. A,* vol. 716, p. 46-53, 2013. doi:10.1016/j.nima.2013.03.061

[12] Yu. Senichev, A. Bogdanov, and R. Maier, "Separatrix formalism for superconducting linear accelerators," *Phys. Rev. ST Accel. Beams, vol. 6*, p. 124001, 2003. doi:10.1103/PhysRevSTAB.6.124001

[13] A. Bartnik *et al.*, "CBETA: First Multipass Superconducting Linear Accelerator with Energy Recovery," *Phys. Rev. Lett,* vol.125, p. 044803, 2020. doi:10.1103/PhysRevLett.125.044803

[14] J. S. Berg *et al.*, "CBETA FFAG Beam Optics Design", in *Proc. ERL'17*, Geneva, Switzerland, Jun. 2017, pp 52-57. doi:10.18429/JACoW-ERL2017-TUIDCC004

[15] R. M. Bodenstein *et al.*, "Current Status of the FFA@CEBAF Energy Upgrade Study", presented at the IPAC'22, Bangkok, Thailand, Jun. 2022, paper THPOST023, this conference.

[16] S. J. Brooks and S. A. Bogacz, "Permanent Magnets for the CEBAF 24GeV Upgrade", presented at the IPAC'22, Bangkok, Thailand, Jun. 2022, paper THPOTK011, this conference.